Egyptian Journal of Medical Research

Print ISSN: 2682-4396 / Online ISSN: 2682-440X

Original article

Role of SERCA and AQP-5 in Diabetes Mellitus-Induced Xerostomia in Adult Male Albino Rat and The Potential Therapeutic Effect of Aldose Reductase Inhibitors: Histological Study

Eman Abas Farag*, Marwa Mohamed Yousry*, Abeer Ibraheem Omar*

*Histology Department, Faculty of Medicine, Cairo University, Egypt**

Article Info

Article history:

Received 29 May 2023

Accepted 28 July 2023

Corresponding Author:

Eman Abas Farag

emanabas@kasralainy.edu.eg

Keywords:

Diabetes-induced xerostomia

polyol pathway

SERCA

AQP-5

Aldose reductase inhibitors

Abstract:

Background: Saliva plays essential roles in different biological processes. Autonomic receptors stimulation is the main regulator of its secretion. Ca^{2+} acts as a 2nd messenger via increasing its cytoplasmic-level (i-Ca^{2+}) &decreasing its endoplasmic reticulum-level (ER-Ca^{2+}) with subsequent protein synthesis as α-amylase and water flow through aquaporin-5 channels (AQP-5). Sarco-ER Ca^{2+}-ATPase (SERCA) pumps i-Ca^{2+} back to ER-Ca^{2+} maintaining low i-Ca^{2+} during rest and allowing its increase during salivary activation. Polyol-pathway overactivity with biological molecules glycation and oxidative-stress is the main mechanism of diabetic complications as xerostomia. As aldose-reductase (AR) is its key-enzyme, multiple AR-inhibitors (ARIs) were newly explored to cure diabetic complications. **Aim of work:** Investigating SERCA &AQP-5 roles in diabetes-induced xerostomia molecular mechanism in

adult male albino rats &the potential ARIs therapeutic effect. **Materials &Methods:** 32 rats were divided into 2 groups: control &experimental [received 55mg/kg streptozotocin to induce diabetes]. 18 hyperglycemic rats were divided into 3 subgroups: diabetic, diabetic/recovery &diabetic/ARIs [received daily oral 57 mg/kg Epalrestat for 4 weeks]. Serum glucose measurement, saliva collection &biochemical, histological, immunohistochemical [for active SERCA, AQP-5, inactive SERCA &caspase-3] and morphometric studies were done. **Results:** All serological, biochemical &histological manifestations of diabetes &xerostomia deteriorated from diabetic subgroup to diabetic/recovery subgroup. However, Epalrestat use evidently improved xerostomia manifestations but not diabetic manifestations. **Conclusion:** The main molecular mechanism of diabetes-induced xerostomia is polyol-pathway overactivity and consequent SERCA inactivation, i-Ca^{2+} overload, ER-stress, AQP-5 reduction, &α-amylase improper folding. Epalrestat, an ARI, ameliorates such xerostomia by blocking this pathway and preventing these changes with no effect on diabetes itself.

1. Introduction:

Saliva has multiple physico-chemical and biological characteristics that allow it to play a vital role in phonation and food tasting, chewing, swallowing and initial food digestion [1]. These functions are achieved by its protein contents which also play a significant immunological function protecting the oral cavity tissues from different bacteria and viruses [2,3].

The main controller of the salivary glands secretion is the autonomic nervous system [sympathetic via noradrenaline (NA) & parasympathetic via acetylcholine (Ach), mainly parasympathetic]. Sympathetic stimulation through binding to β-adrenergic

cell membrane receptors coupled with G-protein increases cyclic adenosine monophosphate (cAMP), intracellular Ca^{2+} and salivary protein synthesis such as amylase-α [4,5].

However, sympathetic, and parasympathetic stimulation of α-adrenergic and muscarinic (M1 & M3) cholinergic plasma membrane receptors, respectively, activate G-protein linked to these receptors and increase inositol triphosphate (IP_3) production. IP_3 binds to its specific receptors (IP3-R) on the endoplasmic reticulum (ER) releasing Ca^{2+} from its ER-stores (ER-Ca^{2+}) to the cytoplasm causing transient increase in the cytosolic Ca^{2+} (i-Ca^{2+}) [2,4,6].

Reduction of ER-Ca^{2+} is detected by stromal interaction molecules (STIMs), an ER-Ca^{2+} binding protein which in turn activates Ca^{2+} channels on the cell membrane allowing entry of the extracellular Ca^{2+}, causing sustained increase in i-Ca^{2+} [7,8]. This mechanism of elevation of i-Ca^{2+} level is called store-operated Ca^{2+} entry (SOCE) [7].

Such way of increase in i-Ca^{2+} acts as signalling messenger that activates translocation of aquaporin-5 (AQP-5) water channels from the endosomes to the acinar apical cell membrane of the salivary glands, increasing its water permeability, water secretion and salivary flow rate [5,9].

Thus, during rest (unstimulated salivary glands), i-Ca^{2+} must be kept at a low-level and ER-Ca^{2+} must be kept at a relative high level to achieve proper increase in i-Ca^{2+} level during autonomic stimulation and ensure efficient intracellular Ca^{2+} signalling [3,6,10,11]. Salivary gland sarco-endoplasmic reticulum Ca^{2+} -ATPase (SERCA2) which pumps Ca^{2+} back from the cytosol to ER-stores and plasma membrane Ca^{2+}-ATPase (PMCA) that pumps Ca^{2+} from the cytoplasm to the extracellular fluid are the two Ca^{2+} channels responsible for achieving this situation [11].

The salivary glands are exocrine glands formed of acini and duct system (intercalated, striated, and excretory) and they are divided into major and minor glands. The major salivary glands are three pairs (parotid, submandibular and sublingual) however, the minor ones are about 600 – 1000 glands widely distributed in the oral submucosa. The parotid gland is the largest major salivary gland, in addition, it is responsible for 25% of the salivary secretion in the unstimulated conditions and accounts for more than 50% of the total saliva with stimulation [12].

Diabetes mellitus is a metabolic disorder leads to hyperglycaemia [13]. Its vigorous spread among the population (more than 400

million adults are affected) [14] increases the incidence of diabetic complications [15,16].

These complications are either of macrovascular or microvascular characteristics. The macrovascular complications comprise cerebrovascular diseases as stroke and cardiovascular diseases like myocardial infarction. But the microvascular complications include other systems affection e.g., diabetic nephropathy, retinopathy, neuropathy, and cataract [17,18].

One of the main molecular mechanisms of these diabetic sequalae is the overactivity of the polyol pathway and uptake of large amount of the extracellular glucose which is present in high level in diabetic patient [14,19]. Basically, Polyol pathway reduces glucose into sorbitol by aldose reductase (AR) using oxidation of NADPH into NADP, then sorbitol is oxidized into fructose by sorbitol dehydrogenase (SDH) using reduction of NAD into NADH [19]. Overactive polyol pathway induces marked decrease in NADPH and NAD with subsequent oxidative stress (OS) [14,19]. It also causes glycation of different cellular molecules such as proteins, lipids and nucleic acids, and formation of advanced glycation end-products (AGEs) with consequent OS [20-22].

Xerostomia (dry mouth) is a common complaint of patients with diabetes mellitus [1,23]. It is caused by salivary glands dysfunction with reduction in the amount of salivary secretion and changes in the salivary contents [5,24]. So, it is manifested by dryness of the oral cavity, and phonation, food tasting & swallowing problems in addition to repeated opportunistic oral and dental infections. All these manifestations lead to poor quality of life of the diabetic patients [1].

Bearing in mind that AR is the first and the rate-limiting enzyme of polyol pathway [19], multiple aldose reductase inhibitors (ARIs) have been recently tested to treat diabetic complications e.g., diabetic nephropathy, retinopathy, neuropathy, cataract [14] and diabetes-induced cardiac complications [25]. Most of these ARIs are still under trials and the only one available in the market is Epalrestat [14].

Aim of work: This work targeted studying the roles of SERCA and AQP-5 in the molecular mechanism of diabetes mellitus-induced xerostomia in adult male albino rats, as well as the possible therapeutic influence of Epalrestat, an example of aldose reductase inhibitors.

2. Materials &Methods:

I) Experimental Design

Thirty-two adult male albino rats (~3 months, ~200 g) were used in this study. The rats were kept in Laboratory Animal

House Unit of Kasr Al-Aini, Faculty of Medicine, Cairo University according to Cairo University-Institutional Animal Care and Use Committee (CU-IACUC) guidelines [approval number CU/III/F/18/23]. All rats were caged under the same environmental conditions for 48 hours before start of the experiment, to adapt to the new environmental conditions. They were supplied with regular chow and water as they needed and housed at 24 ± 1°C in normal light/dark cycle.

The rats were distributed into two principal groups:

Group I (control group, 8 rats):

On the 1st day of the experiment, each rat of this group received 1 ml sodium citrate buffer (0.1 M, pH 4.5) [Sigma-Aldrich, St. Louis, MO, USA]. On day 4, random blood glucose level (RBG) was measured in the blood of the tail vein of each animal using a glucometer (Accu Chek, Roche, Mannheim, Germany) to exclude diabetes. Then they were subdivided into:

- **Subgroup Ia (2 rats):** animals were sacrificed on day 5 with 6 rats of subgroup IIa.
- **Subgroup Ib (6 rats):** each rat was given 1 ml of 1% gum acacia [Sigma-Aldrich, St. Louis, MO, USA] via gastric gavage on daily basis for four weeks (starting from day 5 to day 32 of the experiment). On day 33, all animals of this group were sacrificed with animals of subgroups IIb & IIc.

Group II (experimental group, 24 rats):

On day 1 of the experiment, diabetes was induced in the rats of this group by intraperitoneal (IP) injection of a single dose of 55 mg/kg streptozotocin (STZ) [Sigma-Aldrich, St. Louis, MO, USA] freshly dissolved in 1 ml sodium citrate buffer (0.1 M, pH 4.5) [26]. On day 4, RBG was measured in the blood of the tail vein of each animal to confirm diabetes. Animals had RBG > 300 mg/dl were considered diabetics [9]. Out of these hyperglycemic rats, eighteen were randomly chosen and subdivided equally into:

Subgroup IIa (diabetic subgroup, 6 rats):

On day 5, these rats were sacrificed to ensure the occurrence of diabetes-induced xerostomia and parotid histological changes.

Subgroup IIb (diabetic/recovery subgroup, 6 rats):

Each animal of this subgroup received 1 ml of 1% gum acacia via gastric gavage on daily basis for four weeks (starting from day 5 to day 32 of the experiment). On day 33, all animals of this subgroup were sacrificed.

Subgroup IIc (diabetic/ARIs subgroup, 6 rats):

Each rat received a daily dose of 57 mg/kg of Epalrestat (an ARI) [27] dissolved in 1 ml

of 1% gum acacia via gastric gavage for four weeks (from day 5 to day 32 of the experiment). On day 33, the animals of this subgroup were sacrificed.

II)Animal studies

At each time point (day 5 & day 33), the followings were done in order:

1. **Water intake [28]:** Each rat was allowed water ad libitum from a 250 ml container for 16 h overnight. Accordingly, the amount of water consumed/rat/day was calculated as ml/day.
2. **Urine output [29]:** The 24 h urine for each animal (ml/day) was measured using the metabolic cages with no bedding connecting to a 250 ml container.

   Serological Study:

   Blood samples from the corresponding rats were collected from their tail veins to measure RBG level of at Biochemistry Department, Faculty of Medicine, Cairo University.
3. **Collection of total saliva & measurement of saliva flow rate:**

   At the Laboratory Animal House Unit, the animals were subjected to fasting for two hours, then they were anesthetized by single IP injection of 1 ml/kg ketamine. Pilocarpine hydrochloride (Sigma Chemical Company, St. Louis, MO, USA) in a dose of 0.6 mg/kg was injected IP to stimulate salivation and the **total saliva was collected for 10 min** as follows [9]:

   Dry cotton balls were weighed (weight 1) using electronic balance and kept in the rats' mouths to absorb saliva. After 10 min, these cotton balls were removed and immediately weighed (weight 2) to avoid loss of its moisture. Total saliva flow was calculated in grams by subtracting weight 1 from weight 2 then converted to ml. **The saliva flow rate** was calculated in ml/min by dividing the total saliva by 10.
4. **Measurement of salivary glucose and α-amylase levels [9]:**

   Instantly after saliva collection glucose and α-amylase levels were measured at Biochemistry department, Faculty of Medicine, Cairo University.
5. **Animal sacrifice and measurement of parotid weight:**

   The animals were sacrificed, and the two parotid glands of each animal were dissected and weighed. The right one was sliced and used to prepare parotid homogenate and quantitative real-time polymerase chain reaction (qRT-PCR), while the left one was sliced to prepare paraffin blocks.

III) Parotid Homogenates and enzyme-linked immunosorbent assay (ELISA)

At Biochemistry Department, Faculty of Medicine, Cairo University, parotid homogenates were prepared [30]. Then, according to the manufacturer's instructions, ELISA was done using the suitable antibodies to measure the following values:

- Reactive oxygen species (ROS, oxidizing agent) [MBS166011, MyBioSource, USA].
- Reduced glutathione (GSH, antioxidant) [MBS265966, MyBioSource, USA].

IV) Quantitative real-time polymerase chain reaction (qRT-PCR) [30]

Extraction of the total RNA, synthesis of the complementary DNA and detection of the relative mRNA expression of activating transcription factor-6 (ATF-6, one of the unfolded protein response (UPR) activation markers) were achieved at Biochemistry Department, Faculty of Medicine, Cairo University, using the primers and the Rotor Gene 6000 series software version 1.7 (Corbett Life Science, USA). The results were expressed as a normalized ratio to the internal control, glyceraldehyde-3-phosphate dehydrogenase (GAPDH).

The primer PCR sequences used were:

- ATF-6: Forward 5′-TGGGAGTGAGCTGCAAGTGT-3′
  Reverse 5′-ATAAGGGGGAACCGAGGAG-3′.
- GAPDH: Forward 5′-CTCCCATTCTTCCACCTTTG-3′
  Reverse 5′-CTTGCTCTCAGTATCCTTGC-3′.

V) Histological Study:

Paraffin block preparation:

Fixation of the parotid slices for paraffin blocks preparation was done by keeping them in 10% formol saline for 24 hours. Then, the specimens were processed to paraffin blocks. Sections of six μm-thick were cut and stained with:

1- Hematoxylin and Eosin stain (H&E) [31].

2- Immunohistochemical staining for:

a. **SERCA2 ATPase** [rabbit polyclonal antibody, ab3625, abcam, USA]: it is a specific marker for sarco-endoplasmic reticulum Ca^{2+} ATPase channels in the parotid acinar cells that appears as cytoplasmic reaction.

b. **Aquaporin 5** [rabbit polyclonal antibody, ab 78486, abcam, USA]: AQP-5 water channel marker that appears as an apical membranous reaction in the acinar cells.

c. **Caspase-3** [rabbit polyclonal antibody, ab4051, abcam, USA]:

apoptotic marker appears as a cytoplasmic reaction.

d. SERCA2 C674-SO_3H (sulfonic acid, inactivated SERCA**)** [polyclonal antibody, A300-BL2103, Bethyl Laboratories, USA]. It is a marker for inactive SERCA that appears as cytoplasmic reaction in the acinar cells.

Avidin-biotin technique was used in immunostaining [31], as follows:

- Antigen retrieval of the sections was performed by their boiling in 10 mM citrate buffer (cat no 005000) pH 6 for 10 min.
- The sections were then cooled at room temperature for 20 min.
- Incubation of the sections with the primary antibodies for one hour was done.
- Then, immunostaining was completed using Ultravision One Detection System (cat no TL - 060- HLJ) and Lab Vision Mayer's hematoxylin counterstaining (cat no TA- 060- MH).

Preparation of the negative control sections was done by the same process after omission of the primary antibodies.

Citrate buffer, Ultravision One Detection System and Ultravision Mayer's hematoxylin were purchased from Labvision, ThermoFisher scientific, USA.

VI) Morphometric study

The area percent of the positive immuno-reaction for SERCA2, AQP-5, caspase-3 and SERCA2 C674-SO_3H were measured in the corresponding immunostained sections in ten non-overlapping fields for each rat in each group (×100).

Leica Qwin-500 LTD-software image analysis computer system (Cambridge, England) was used for image analysis.

VII) Statistical analysis

Using IBM Statistical Package for the Social Sciences (SPSS) version 21, all biochemical and morphometric results were expressed as mean ± standard deviation (SD). Then, their statistical analysis was accomplished using one-way analysis of variance (ANOVA) and "Tukey" post hoc test. The results were considered statistically significant when P value was < 0.05.

All the histological and morphometric studies, in addition to the statistical analysis were done at Histology Department, Faculty of Medicine, Cairo University.

3. Results:

General observations

- No deaths were observed in all experimental rats.
- Animals of subgroups Ia & Ib showed similar serological, biochemical, and

histological results. So, they were collectively described as control group (group I).

- After confirmation of diabetes, polydipsia and polyuria were detected as follows:

- Water intake **[Fig. 1a]** showed significant increase in subgroups IIa & IIb versus control group and in subgroup IIb versus subgroup IIa. However, in subgroup IIc, it revealed significant decrease compared to subgroup IIb and non-significant increase compared to control group.
- Urine output **[Fig. 1a]** revealed significant increase in subgroups IIa, IIb & IIc in comparison with control group. Additionally, it showed significant increase in subgroup IIb versus IIa and non-significant decrease in subgroup IIc versus subgroup IIb.

Animal Data

Serological Results [Fig. 1b]:

RBG level showed significant increase in subgroups IIa and IIb in comparison with group I and in subgroup IIb with subgroup IIa. On the other hand, its level demonstrated non-significant decrease in subgroup IIc compared to subgroup IIb and significant increase compared to group I.

Saliva flow rate [Fig. 1c]:

It revealed significant decrease in subgroups IIa and IIb compared to group I and in subgroup IIb compared to subgroup IIa. Conversely, its level in subgroup IIc showed significant increase compared to subgroup IIb and non-significant decrease compared to group I.

Salivary glucose & α-amylase levels [Figs. 1c & 1d]:

Salivary glucose and α-amylase expressed statistical analysis results like those of serum glucose and salivary flow rate, respectively.

Parotid weight [Fig. 1e]:

It showed non-significant decrease in subgroups IIa, IIb & IIc when compared to control group. In addition, there was non-significant decrease between the mean parotid weights of subgroup IIb versus subgroup IIa and non-significant increase between subgroup IIc and subgroup IIb.

ELISA Results for ROS & GSH and qRT-PCR results for ATF-6 [Figs. 1f & 1g]:

ROS level & ATF-6 mRNA expression revealed significant increase in subgroups IIa & IIb compared to group I and in subgroup IIb compared to subgroup IIa. In subgroup IIc, they demonstrated significant decrease versus subgroup IIb and non-significant increase versus group I. Conversely, GSH level exhibited significant decrease in subgroup IIa & subgroup IIb in comparison with group I and in subgroup IIb in comparison with subgroup IIa. However,

it showed significant increase in subgroup IIc versus subgroup IIb and non-significant decrease versus group I.

Histological Results:

H&E-stained sections:

In **group I (control group) [Figs. 2a & 2b]**, the parotid gland appeared formed of multiple lobes and lobules with delicate connective tissue (CT) septa in-between. It showed multiple pure serous acini that were tightly packed and a duct system that consisted of intralobular and excretory ducts. The intralobular ducts included striated ducts, the most obvious intralobular ducts, and the intercalated ducts that scarcely seen as they were compressed in-between the acini.

However, in **subgroup IIa (diabetic subgroup) [Figs. 2c, 2d],** some of the acinar and duct cells showed darkly stained shrunken nuclei together with cytoplasmic vacuolations. The CT septa showed few vacuolations and scattered few mononuclear inflammatory cells.

Subgroup IIb (diabetic/recovery subgroup) [Figs. 2e, 2f, 2g] showed progression of the degenerative and the inflammatory features detected in subgroup IIa (diabetic subgroup). Most of the acinar and duct cells revealed shrunken darkly stained nuclei and marked cytoplasmic vacuolations. In addition, the CT septa appeared with marked vacuolations, dilated and congested blood vessel and heavy mononuclear inflammatory cell infiltration.

In **subgroup IIc (diabetic/ARIs subgroup) [Figs. 2h, 2i],** the parotid glands showed marked improvement of the degenerative and the inflammatory signs associated with diabetes where their sections demonstrated nearly normal features except for the presence of few shrunken dense nuclei in the acinar & duct cells and very few inflammatory cells. However, there was persistence of the cytoplasmic and CT vacuolations.

In SERCA2 ATPase immunostained sections of:

Group I (control group) [Fig. 3a], the positive immunoreaction was copious in almost all acinar cells' cytoplasm. While in **subgroup IIa (diabetic subgroup) [Fig. 3b],** this acinar cells' positive immunoreaction was decreased, to be detected in few parotid acinar cells in **subgroup IIb (diabetic/recovery subgroup) [Fig. 3c]**. However, **subgroup IIc (diabetic/ARIs subgroup) [Fig. 3d]** displayed such positive cytoplasmic immunoreaction in most of the parotid acinar cells.

AQP-5 immunostained sections of:

Control group (group I) [Fig. 4a] showed abundant membranous positive

immunostaining in the apical cell membranes of the acinar cells. Such immunoreaction was visualized to be less abundant in **diabetic subgroup (subgroup IIa) [Fig. 4b]** and scanty in **diabetic/recovery subgroup (subgroup IIb) [Fig. 4c]. In diabetic/ARIs subgroup (subgroup IIc) [Fig. 4d],** it proved widespread.

In caspase-3 immunostained sections of:

Group I (control group) [Fig. 5a], there was few positive immunoreaction throughout the cytoplasm of the acinar cells of the parotid glands.

Such immunopositive reaction demonstrated increase in the cytoplasm of the parotid acinar cells in **subgroup IIa (diabetic subgroup) [Fig. 5b]** and wide distribution in **subgroup IIb (diabetic/recovery subgroup) [Fig. 5c]**. Then, it revealed marked regression in **subgroup IIc (diabetic/ARIs subgroup) [Fig. 5d]**.

SERCA2 C674-SO_3H immunostained sections:

In **control group (I) [Fig. 6a],** exhibited barely dispersed positive cytoplasmic immunostaining in the parotid acinar cells. In **diabetic subgroup (IIa) [Fig. 6b],** the positive reaction revealed increase in distribution to become extensively disseminated in **diabetic/recovery subgroup (IIb) [Fig. 6c]**. Then again in **diabetic/ARIs subgroup (IIc) [Fig. 6d],** it was scarcely distributed.

Morphometric Results:

Statistically, the mean area percent of SERCA2 ATPase (active SERCA) **[Fig. 3e]** & AQP-5 **[Fig. 4e]** positive immunoreactions denoted significant decrease in subgroups IIa and IIb versus group I and significant decrease in subgroup IIb versus subgroup IIa. Moreover, subgroup IIc showed significant increase versus subgroup IIb and non-significant decrease versus group I.

Regarding statistical analysis of the positive immunoreaction mean area percent of caspase-3 **[Fig. 5e]** & SERCA2 C674-SO_3H (inactive SERCA) **[Fig. 6e]**, there were significant increase in subgroup IIa and subgroup IIb compared to group I and in subgroup IIb compared to subgroup IIa. While in subgroup IIc, there were significant decrease versus subgroup IIb and non-significant increase versus group I.

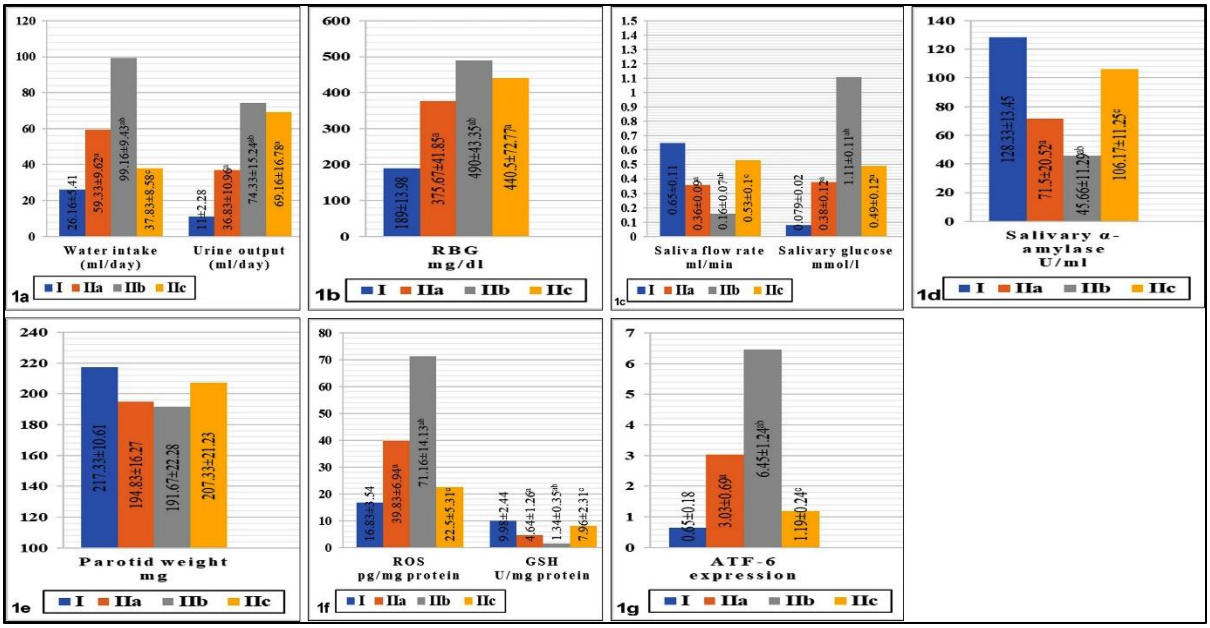

Fig. 1: Showing the mean values of: 1a: Water intake &Urine output. **1b:** RBG level. **1c:** Saliva flow rate & salivary glucose. **1d:** Salivary α-amylase level. **1e:** Parotid weight. **1f:** ELISA levels for parotid homogenate ROS & GSH. **1g:** qRT-PCR expression for parotid ATF-6.

[^{a} as compared to group I, ^{b} as compared to subgroup IIa & ^{c} as compared to subgroup IIb (significant difference at $P < 0.05$)]

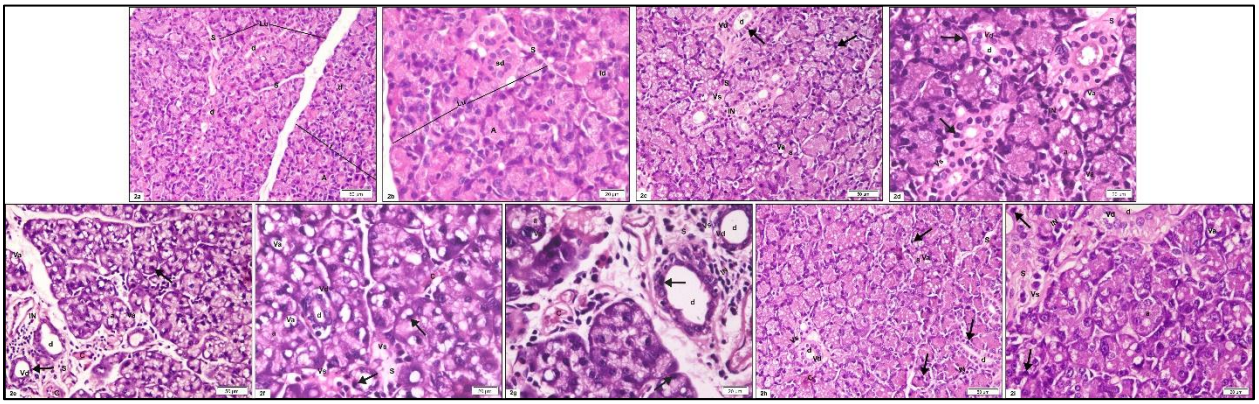

Fig. 2: Photomicrographs of H&E-stained sections in the parotid gland: 2a & 2b (the control group, group I): The parotid gland is formed of multiple lobes (L) and lobules (Lu) separated by connective tissue septa (S). Tightly packed serous acini (A) and a duct system (d) [striated ducts (sd) &intercalated ducts (id)] are seen. **2c & 2d (diabetic subgroup, subgroup IIa):** Some of the acinar (a) and duct (d) cells reveal darkly stained shrunken nuclei (arrows). Besides, few inflammatory cells (IN) are observed in the CT septa (S). Also, there are cytoplasmic vacuolations in some acinar cells (Va) and some duct cells (Vd). Few vacuolations (Vs) are seen in the CT septa. **2e, 2f & 2g (diabetic/recovery subgroup, subgroup IIb):** Most of the acinar (a) and duct (d) cells are illustrating shrunken darkly stained nuclei (arrows). Additionally, marked cytoplasmic vacuolations are visualized in most of the acinar cells (Va) and duct cells (Vd). Dilated and congested blood vessels (C), marked vacuolations (Vs) and intense mononuclear inflammatory cell infiltration (IN) are clearly seen in the CT septa (S). **2h & 2i (diabetic/ARIs subgroup, subgroup IIc):** The parotid gland has nearly normal histological features. But there are few shrunken dense nuclei (arrows) in the acinar (a) & duct cells (d) in addition to mild blood vessels congestion (C) and few inflammatory cells (IN) in the CT septa (S). Persistence of vacuolations is observed in acinar cells (Va), duct cells (Vd) and CT septa (Vs). **[2a, 2c, 2e & 2h: H&E, x200; 2b, 2d, 2f, 2g & 2i: H&E, x400]**

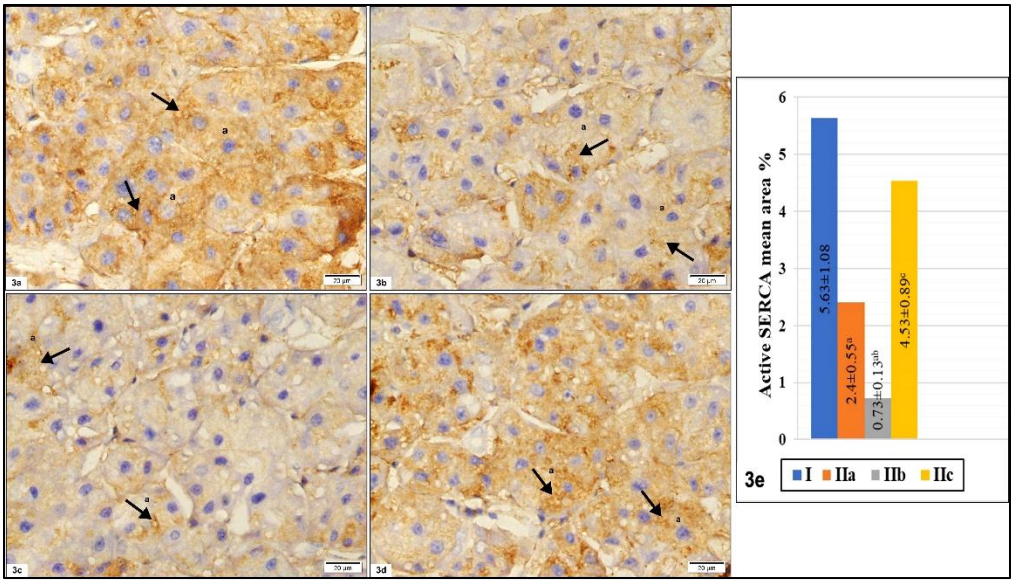

Fig. 3: Photomicrographs of SERCA2 ATPase immunostained sections in the parotid gland [anti SERCA2 ATPase immunohistochemical stain, x400]: 3a (the control group, group I): Abundant positive cytoplasmic immunoreaction (arrows) in almost all acinar cells (a) is detected. **3b (diabetic subgroup, subgroup IIa):** Decreased positive cytoplasmic immunoreaction (arrows) in the majority of acinar cells (a) is seen. **3c (diabetic/recovery subgroup, subgroup IIb):** positive cytoplasmic immunoreaction (arrows) is only observed in few acinar cells (a). **3d (diabetic/ARIs subgroup, subgroup IIc):** Profuse positive cytoplasmic immunoreaction (arrows) in most of the acinar cells (a) is demonstrated. **3e:** Showing **the mean area % of active SERCA2 ATPase** positive cells.

[^{a} as compared to group I, ^{b} as compared to subgroup IIa & ^{c} as compared to subgroup IIb (significant difference at $P < 0.05$)]

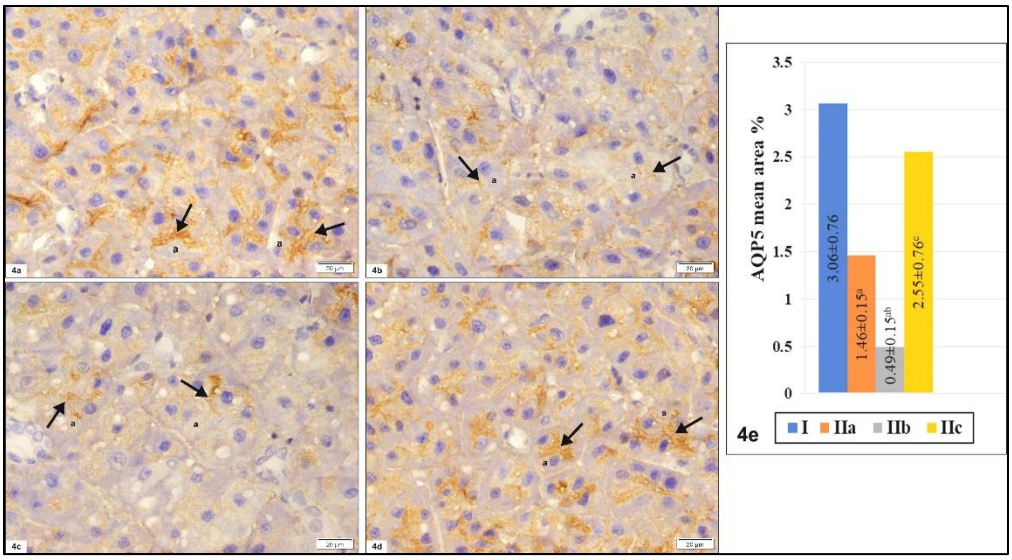

Fig. 4: Photomicrographs of AQP-5 immunostained sections in the parotid gland [anti AQP-5 immunohistochemical stain, x400]: 4a (the control group, group I): There is copious membranous positive immunostaining in the apical cell membranes (arrows) in almost all acinar cells (a). **4b (diabetic subgroup, subgroup IIa):** Some positive immunoreactivity in the apical cell membranes (arrows) of acinar cells (a) can be visualized. **4c (diabetic/recovery subgroup, subgroup IIb):** Scanty disseminated positive immunoreactivity is noticed in the apical cell membranes (arrows) of acinar cells (a). **4d (diabetic/ARIs subgroup, subgroup IIc):** There is widespread membranous positive immunoreaction in the apical cell membranes (arrows) of most of the acinar cells (a). **4e:** Showing **the mean area % of AQP-5** positive cells.

[^{a} as compared to group I, ^{b} as compared to subgroup IIa & ^{c} as compared to subgroup IIb (significant difference at $P < 0.05$)]

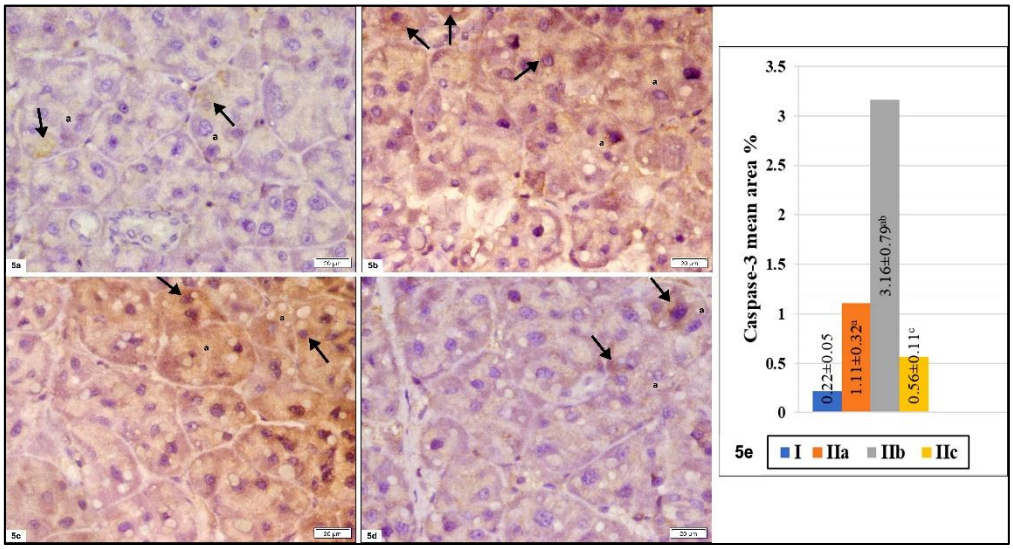

Fig. 5: Photomicrographs of caspase-3 immunostained sections in the parotid gland [anti caspase-3 immunohistochemical stain, x400]: 5a (the control group, group I): Few positive cytoplasmic immunoreactions (arrows) are observed in few acinar cells (a). **5b (diabetic subgroup, subgroup IIa):** Cytoplasmic immunoreaction (arrows) is observed in many acinar cells (a).

5c (diabetic/recovery subgroup, subgroup IIb): Widely spread cytoplasmic immunoreactivity (arrows) is seen in many acinar cells (a). **5d (diabetic/ARIs subgroup, subgroup IIc):** The presence of scanty cytoplasmic immunoreaction (arrows) can be noticed in few acinar cells (a). **5e:** Showing **the mean area % of caspase-3** positive cells.

[^{a} as compared to group I, ^{b} as compared to subgroup IIa & ^{c} as compared to subgroup IIb (significant difference at $P < 0.05$)]

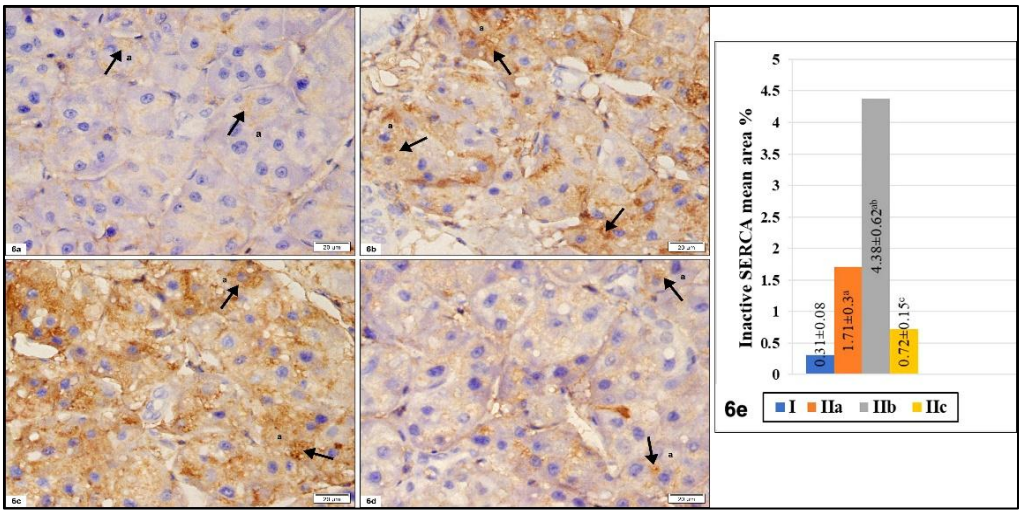

Fig. 6: Photomicrographs of SERCA2 C674-SO_3H immunostained sections in the parotid gland [anti SERCA2 C674-SO_3H immunohistochemical stain, x400]: 6a (the control group, group I): Scarcely dispersed positive cytoplasmic immunoreaction (arrows) is seen in acinar cells (a). **6b (diabetic subgroup, subgroup IIa):** Marked positive cytoplasmic immunoreaction (arrows) can be seen in most of the acinar cells (a). **6c (diabetic/recovery subgroup, subgroup IIb):** Extensive positive cytoplasmic immunoreactions (arrows) are noted in acinar cells (a). **6d (diabetic/ARIs subgroup, subgroup IIc):** Barely distributed positive cytoplasmic immunoreactivity (arrows) is noted in few acinar cells (a). **6e:** Showing **the mean area % of SERCA2 C674-SO_3H** positive cells.

[^{a} as compared to group I, ^{b} as compared to subgroup IIa & ^{c} as compared to subgroup IIb (significant difference at $P < 0.05$)]

4. Discussion:

Diabetes mellitus is a worldwide metabolic disturbance where insulin is either not sufficiently secreted by β-cells of pancreas (type I) or not properly functioning due to its receptors resistance (type II) [13]. It is expected that diabetes will affect more than 600 million by year 2040 [14]. This increases the incidence of morbidities and mortalities caused by its complications [15,16]. Xerostomia, one of the commonest diabetic complications, results from malfunction of the salivary glands with subsequent change in the saliva composition and/or decrease in its amount. Such malfunction is followed by

multiple morbidities with poor quality of life [1,5,23,24].

The parotid gland was selected for this study as it is the largest major salivary gland. Moreover, it contributes largely to salivary secretion (form 25% in unstimulated conditions up to 50% in the active state) [12].

Throughout this work the roles of SERCA and AQP-5 in the molecular mechanism of diabetes mellitus-induced xerostomia in adult male albino rats, as well as the possible therapeutic influence of Epalrestat (an aldose reductase inhibitor) were investigated.

Calcium ions play a vital role in maintaining the integrity and the function of the endoplasmic reticulum (ER). They regulate the post translational processing and the protein folding via conserving the balance between translocated secretory protein to ER and its folding. This is achieved by the presence of optimum level of ER-Ca^{2+} [9].

Moreover, in the salivary glands under the effect of autonomic stimulation, Ca^{2+} acts as second messenger in the process of salivary secretion of water and proteins such as α-amylase via the rapid sustained increase of its intracellular level [5,9]. Such results were achieved in this study via IP injection of pilocarpine similar to what was reported formerly [9] where pilocarpine stimulates the release of acetyl Choline (ACh) that in turn, activates the muscarinic receptors (M1 & M3).

The rats of subgroup IIa in this study (diabetic subgroup) showed significant increase in mean RBG level versus control group. This ensured persistent hyperglycaemia till time of their sacrifice similar to what was reported in a previous study [9]. Such high blood glucose is followed by increased glucose secretion in saliva which is backed in this subgroup by the significant increase in salivary glucose level when compared to that in control group. In addition, rats of subgroup IIa showed polyuria which could be enlightened by the secretion of glucose in urine accompanied by its osmotic water due to increased plasma glucose level above renal threshold [32].

These rats also revealed manifestations of salivary dysfunction such as decreased salivary α-amylase which could be explained by polyol pathway activation induced by hyperglycaemia [14,19]. Throughout this pathway high glucose level is reduced into sorbitol by AR then sorbitol is oxidized into fructose by SDH [33]. High level of fructose induces protein glycation through increasing the glycation agents and change of fructose to acetyl COA after consumption of ATP [34]. Glycation of SERCA2 in the salivary glands results in its

inactivation which was proved in this group by the significant decrease in the mean area percent of SERCA2 ATPase positive immunoreaction and the significant increase in that of SERCA2 C674-SO_3H **(**sulfonic acid, inactivated SERCA) compared to the control group.

Bearing in mind that SERCA is a major regulator of ER-Ca^{2+} and i-Ca^{2+} optimum levels via pumping of Ca^{2+} during rest from the cytoplasm of the salivary gland acinar cells to their ER maintaining low i-Ca^{2+} and relative high ER-Ca^{2+} [5]. Glycated inactivated SERCA in group II of this study (experimental group) was assumed to cause low level of ER-Ca^{2+} with consequent ER stress and improper post translational protein processing and folding which eventually decreased salivary protein synthesis as α-amylase. Such assumption was documented by the significant increase in RNA expression of ATF-6 in this group versus group I (control group).

Another consequence of the parotid gland dysfunction reported in diabetic subgroup (IIa) of this work was the significant decrease in the mean area percent of AQP-5 positive immunoreaction compared with that of group I. This finding could be elucidated by inefficient folding of AQP-5 protein channels due to induced ER stress by SERCA glycation and inactivation. Another explanation could be the insufficient translocation of these channels to the apical cell membranes [5,9]. This diminished translocation was presumed to result from improper intracellular Ca^{2+} signalling where diabetes-induced inactivated SERCA increased i-Ca^{2+} and decreased ER- Ca^{2+} preventing the initial transient and the subsequent rapid sustained increase in i-Ca^{2+}. In addition, hyperglycaemia was proved to decrease sensitivity of IP3R on ER decreasing the release of Ca^{2+} [11].

Parotid gland dysfunction in diabetic subgroup IIa was also manifested by significantly decreased saliva flow rate versus control group. These findings could be clarified by the proved decrease in salivary protein (α-amylase) synthesis and the reduced salivary water secretion resulted from documented decreased AQP-5 expression.

Diminished salivary water secretion was also suggested to be due to the osmotic power of high level of intracellular glucose [14] keeping water intracellularly and preventing its secretion. Such suggestion was defended in subgroup IIa by the presence of cytoplasmic and CT vacuoles in the parotid gland. This finding was previously stated in submandibular gland following induction of diabetes [9]. Reduced salivary water content with the resultant

xerostomia could be the cause of the polydipsia (pathological thirst) observed in diabetic subgroup of this study that might occur as a compensatory mechanism [9].

Moreover, diabetic subgroup (IIa) of this work revealed a significant increase in the parotid homogenate ROS level and a significant decrease in GSH level when compared to those in the control group. These findings were assumed to result from diabetes-induced overactivation of polyol pathway that provokes a marked reduction in NADPH and an increase in $NADP^+$ during the reduction of glucose into sorbitol. Decreased NADPH lowers the production of GSH (the antioxidant that binds the free radicals & H_2O_2) as it is needed for GSH/GSH disulfide balance [35]. Furthermore, oxidation of sorbitol into fructose consumes NAD^+ and increases NADH. This redox imbalance increases the electron transport in mitochondrial electron transport chain and increases the production of ROS [34]. In addition, the increased i-Ca^{2+} induced by inactivated SERCA increases mitochondrial Ca^{2+} that increases the production of mitochondrial ROS [36].

The oxidant/antioxidant imbalance results in OS that is followed by inflammatory reaction and apoptotic cell death [37]. These results were demonstrated in the histological sections of subgroup IIa of the current study and enforced by the significant increase in caspase-3 mean area percent in this subgroup versus control group (I).

Apoptosis could also be explained by sequalae of polyol pathway overactivation such as: decreased ATP production because of NAD^+/NADH imbalance that inhibits glycolysis and Kreb's cycle, increased ATP consumption during conversion of fructose into acetyl COA and cellular protein glycation induced by fructose [14]. ER stress and the release of UPR such as IRE1(inositol-requiring kinase 1), PERK (double-stranded RNA-activated protein kinase -like endoplasmic reticulum kinase) & ATF-6 could also add to the inflammatory and the apoptotic response according to the severity of ER stress [38].

Apoptosis and salivary gland dysfunction with subsequent reduction in α-amylase and water production observed in this subgroup (IIa) could rationalize the decrease in the parotid weight. However, this reduction did not show significant decrease when compared to that of the control group. Such finding was supposed to be due to inflammatory cells infiltration and intracellular and CT accumulation of water vacuoles.

The subgroup IIb of the current study (diabetic/recovery subgroup) clarified persistence and worsening of all

biochemical, histological, and statistical results when compared with those of subgroup IIa (diabetic subgroup). This could be enlightened by the continuance elevation of the blood glucose level caused by the permanent and the progressive pancreatic β-cells lesion induced by STZ [39].

Oral administration of Epalrestat (ARI) for 4 weeks after induction of diabetes in subgroup IIc (diabetic/ARIs subgroup) induced obvious amelioration of the diabetic effects on parotid gland. There was marked significant decrease in water intake in the animals of this subgroup compared to diabetic/recovery subgroup (IIb). This improvement could be clarified by the regression of xerostomia because of the detected significant increase in the mean area percent of AQP-5 immunoreaction versus subgroup IIb and its non-significant decrease versus control group with subsequent increase in the salivary water content.

Increased expression of AQP-5 was presumed to be a sequalae of recovering of proper i-Ca^{2+} level and its sufficient use as 2^{nd} messenger. This was supported by the previously reported improvement of the cardiac contractile dysfunction in diabetic rats' hearts following the inhibition of AR [40]. This assumption was also reinforced by the significant increase in the mean area percent of SERCA2 immuno-expression and significant decrease in that of the inactive SERCA versus subgroup IIb and their non-significant change versus control group.

These findings were suggested to be followed by regression of the ER stress as reviewed previously [41]. Such suggestion was confirmed by the significant decrease in ATF-6 RNA expression in this subgroup compared to subgroup IIb and its non-significant increase compared to control group (I). Consequently, there was proper folding of α-amylase and increase in its salivary secretion confirmed by the significant increase in its level in diabetic/ARIs subgroup (IIc) versus diabetic/recovery subgroup (IIb) and its non-significant decrease versus control group, in addition to the proper folding of AQP-5 channels that added to the significant increase in its immunoreaction mean area percent. Increase in the salivary content of water and α-amylase resulted into significant increase in the salivary flow rate versus subgroup IIb and their non-significant decrease versus control group.

The almost normalization of SERCA2 activity was assumed to result from decreased its glycation by the products of polyol pathway. As the use of Epalrestat inhibited aldose reductase which the key enzyme for this pathway with subsequent

decrease in intracellular level of sorbitol, fructose and NADH and increase in the that of NADPH and NAD^+. Such rebalancing was followed by amelioration of OS [14] which was supported in this subgroup by significant decrease in the ROS and significant increase in GSH levels compared to their levels in subgroup IIb and the non-significant changes in their levels compared to control group.

Decreased OS and ER stress were followed by decreased inflammatory reaction, inflammatory cell infiltration and apoptosis [42,43]. These findings were detected histologically in this subgroup. In addition, amelioration of apoptosis was reinforced by the significant decrease in the mean area percent of caspase-3 positive reaction and its non-significant increase when compared to diabetic/recovery subgroup and control group, respectively.

Surprisingly, such improvement induced by Epalrestat (ARI) was limited only to the manifestations of xerostomia produced by diabetes in the parotid gland without any advance in the diabetes as a disease. This was defended in diabetic/ARIs subgroup (IIc) of this work by the persistent cytoplasmic and CT vacuolations and the persistent significant increase in the urine output, RBG & salivary glucose level when compared to those in control group, in addition to their non-significant decrease when compared with diabetic/recovery subgroup (IIb). Further support came from the non-significant change in the mean parotid weight throughout the experiment compared to the control group based on the compensation between deceased weight by apoptosis and increased weight by persistence of vacuolations and inflammatory cell infiltration.

This might be explained by that inhibition of polyol pathway activity via AR inhibition was followed by over accumulation of glucose in the tissues. This, in turn, resulted into persistence of the diabetic manifestations and limitation of the improvement to the diabetic complications provoked by polyol pathway activation.

5. Conclusion:

From this work, it can be concluded that SERCA2 inactivation via polyol pathway overactivation was the main cause of diabetes-induced xerostomia, a common complication of diabetes. This was achieved through inefficient i-Ca^{2+} level, ER stress with subsequent α-amylase & AQP-5 improper folding, ineffective Ca^{2+} signalling and the consequent decreased AQP-5 apical translocation, in addition to OS, inflammatory reactions and apoptosis. All

these manifestations could be stopped by the inhibition of AR, the key enzyme in polyol pathway, by the oral use of Epalrestat (an ARI). Moreover, Epalrestat was not effective in the treatment of diabetes itself but effective in the treatment of one of its main complications, the conclusion which needs more investigations.

Conflict of interests: There are no conflicts of interest.

6. References:

1- Aitken-Saavedra J, Rojas-Alcayaga G, Maturana-Ramírez A, Escobar-Álvarez A, Cortes-Coloma A, Reyes-Rojas M, Viera-Sapiain V, Villablanca-Martínez C, Morales-Bozo I. Salivary gland dysfunction markers in type 2 diabetes mellitus patients. J Clin Exp Dent. 2015; 7: e501-5.

2- Ambudkar IS. Ca^{2+} signaling and regulation of fluid secretion in salivary gland acinar cells. Cell Calcium. 2014; 55:297-305.

3- Ambudkar IS. Calcium signalling in salivary gland physiology and dysfunction. J Physiol. 2016; 594:2813-24.

4- Pedersen AML, Sørensen CE, Proctor GB, Carpenter GH, Ekström J. Salivary secretion in health and disease. J Oral Rehabil. 2018; 45:730-46.

5- Ambudkar I. Calcium signaling defects underlying salivary gland dysfunction. Biochim Biophys Acta Mol Cell Res. 2018; 1865:1771-7.

6- Ambudkar IS. Regulation of calcium in salivary gland secretion. Crit Rev Oral Biol Med. 2000; 11:4-25.

7- Liu X, Cheng KT, Bandyopadhyay BC, Pani B, Dietrich A, Paria BC, Swaim WD, Beech D, Yildrim E, Singh BB, Birnbaumer L, Ambudkar IS. Attenuation of store-operated Ca2+ current impairs salivary gland fluid secretion in TRPC1(-/-) mice. Proc Natl Acad Sci U S A. 2007; 104:17542-7.

8- Hong JH, Li Q, Kim MS, Shin DM, Feske S, Birnbaumer L, Cheng KT, Ambudkar IS, Muallem S. Polarized but differential localization and recruitment of STIM1, Orai1 and TRPC channels in secretory cells. Traffic. 2011; 12:232-45.

9- Bhattarai KR, Lee HY, Kim SH, Kim HR, Chae HJ. Ixeris dentata Extract Increases Salivary Secretion through the Regulation of Endoplasmic Reticulum Stress in a Diabetes-Induced Xerostomia Rat Model. Int J Mol Sci. 2018; 19:1059.

10- Melvin JE, Yule D, Shuttleworth T, Begenisich T. Regulation of fluid and electrolyte secretion in salivary gland acinar cells. Annu Rev Physiol. 2005; 67:445-69.

11- Fedirko NV, Kruglikov IA, Kopach OV, Vats JA, Kostyuk PG, Voitenko NV. Changes in functioning of rat submandibular salivary gland under streptozotocin-induced diabetes are associated with alterations of Ca2+ signaling and Ca2+ transporting pumps. Biochim Biophys Acta. 2006; 1762:294-303.

12- Pedersen A, Sørensen CE, Proctor GB, Carpenter GH. Salivary functions in mastication, taste and textural perception, swallowing and initial digestion. Oral Dis. 2018; 24:1399-1416.

13- American Diabetes Association. Diagnosis and classification of diabetes mellitus. Diabetes Care. 2014; 37 1: S81-90.

14- Thakur S, Gupta SK, Ali V, Singh P, Verma M. Aldose Reductase: a cause and a potential target for the treatment of diabetic complications. Arch Pharm Res. 2021; 44:655-67.

15- Demir Y, Taslimi P, Koçyiğit ÜM, Akkuş M, Özaslan MS, Duran HE, Budak Y, Tüzün B, Gürdere MB, Ceylan M, Taysi S, Gülçin İ, Beydemir Ş. Determination of the inhibition profiles of pyrazolyl-thiazole derivatives against aldose reductase and α-glycosidase and molecular docking studies. Arch Pharm (Weinheim). 2020; 353: e2000118.

16- Taslimi P, Aslan HE, Demir Y, Oztaskin N, Maraş A, Gulçin İ, Beydemir S, Goksu S. Diarylmethanon, bromophenol and diarylmethane compounds: Discovery of potent aldose reductase, α-amylase and α-glycosidase inhibitors as new therapeutic approach in diabetes and functional hyperglycemia. Int J Biol Macromol. 2018; 119:857-63.

17- Chawla A, Chawla R, Jaggi S. Microvasular and macrovascular complications in diabetes mellitus: Distinct or continuum? Indian J Endocrinol Metab. 2016; 20:546-51.

18- Grewal AS, Bhardwaj S, Pandita D, Lather V, Sekhon BS. Updates on Aldose Reductase Inhibitors for Management of Diabetic Complications and Non-diabetic Diseases. Mini Rev Med Chem. 2016; 16:120-62.

19- Jannapureddy S, Sharma M, Yepuri G, Schmidt AM, Ramasamy R. Aldose Reductase: An Emerging Target for Development of Interventions for Diabetic Cardiovascular Complications. Front Endocrinol (Lausanne). 2021; 12:636267.

20- Litwinoff E, Hurtado Del Pozo C, Ramasamy R, Schmidt AM. Emerging Targets for Therapeutic Development in Diabetes and Its Complications: The

RAGE Signaling Pathway. Clin Pharmacol Ther. 2015; 98:135-44.

21- Ruiz HH, Ramasamy R, Schmidt AM. Advanced Glycation End Products: Building on the Concept of the "Common Soil" in Metabolic Disease. Endocrinology. 2020; 161: bqz006.

22- Egaña-Gorroño L, López-Díez R, Yepuri G, Ramirez LS, Reverdatto S, Gugger PF, Shekhtman A, Ramasamy R, Schmidt AM. Receptor for Advanced Glycation End Products (RAGE) and Mechanisms and Therapeutic Opportunities in Diabetes and Cardiovascular Disease: Insights From Human Subjects and Animal Models. Front Cardiovasc Med. 2020; 7:37.

23- Bhattarai KR, Junjappa R, Handigund M, Kim HR, Chae HJ. The imprint of salivary secretion in autoimmune disorders and related pathological conditions. Autoimmun Rev. 2018; 17:376-90.

24- Nanci A. Salivary Glands. In Ten Cate's Oral Histology: Development, Structure, and Function (Ninth Edition), Elsevier,2016, pp: 536-88.

25- Johnson BF, Nesto RW, Pfeifer MA, Slater WR, Vinik AI, Chyun DA, Law G, Wackers FJ, Young LH. Cardiac abnormalities in diabetic patients with neuropathy: effects of aldose reductase inhibitor administration. Diabetes Care. 2004; 27:448-54.

26- Padugupati S, Ramamoorthy S, Thangavelu K, Sarma D, Jamadar D. Effective Dose of Streptozotocin to Induce Diabetes Mellitus and Variation of Biophysical and Biochemical Parameters in Albino Wistar Rats. J Clin of Diagn Res. 2021; 15: BF01-BF05.

27- Jaiswal S, Ss T, Mishra S. Neuroprotective effect of Epalrestat on memory impairment in streptozotocin-induced type-2 diabetic rats using different behavioral models. Asian J Pharm Clin Res. 2018; 11: 411–5.

28- Cassandra R. Stewart, Nneka Obi, Elodie C. Epane , Alexander A. Akba , Leslie Halpern, Janet H. Southerland, Pandu R. Gangula. The Effects of Diabetes on Salivary Gland Protein Expression of Tetrahydrobiopterin and Nitric Oxide Synthesis and Function. J Periodontol. 2016; 87: 735–41.

29- Turner T, Chen X, Zahner M, Opsahl A, DeMarco G, Boucher M, Goodwin B, Perreault M. FGF21 increases water intake, urine output and blood pressure in rats. PLoS ONE. 2018; 14;13: e0202182.

30- El Agaty SM. Cardioprotective effect of vitamin D2 on isoproterenol-induced myocardial infarction in diabetic rats.

Archives of Physiology and Biochemistry. 2019; 125:210-9.

31- Suvarna K, Layton C, Bancroft J. The hematoxylins and eosin& Immunohistochemical techniques. In Bancroft's Theory and Practice of Histological Techniques (Eighth Edition), Elsevier,2019, pp: 126-38 & 337-94.

32- Yue XD, Wang JY, Zhang XR, Yang JH, Shan CY, Zheng MY, Ren HZ, Zhang Y, Yang SH, Guo ZH, Chang B, Chang BC. Characteristics and Impact Factors of Renal Threshold for Glucose Excretion in Patients with Type 2 Diabetes Mellitus. J Korean Med Sci. 2017; 32:621-7.

33- Mathebula SD. Polyol pathway: A possible mechanism of diabetes complications in the eye. Afr. Vision Eye Health. 2015;74: 5 pages.

34- Yan LJ. Redox imbalance stress in diabetes mellitus: Role of the polyol pathway. Animal Model Exp Med. 2018; 1:7-13.

35- Shen H, Wang W. Effect of glutathione liposomes on diabetic nephropathy based on oxidative stress and polyol pathway mechanism. J Liposome Res. 2021; 31:317-25.

36- Duchen MR. Roles of mitochondria in health and disease. Diabetes. 2004; 53:S96-102.

37- Jian Z, Guo H, Liu H, Cui H, Fang J, Zuo Z, Deng J, Li Y, Wang X, Zhao L. Oxidative stress, apoptosis and inflammatory responses involved in copper-induced pulmonary toxicity in mice. Aging (Albany NY). 2020; 12:16867-86.

38- Chaudhari N, Talwar P, Parimisetty A, Lefebvre d'Hellencourt C, Ravanan P. A molecular web: endoplasmic reticulum stress, inflammation, and oxidative stress. Front Cell Neurosci. 2014; 8:213.

39- Cruz PL, Moraes-Silva IC, Ribeiro AA, Machi JF, de Melo MDT, Dos Santos F, da Silva MB, Strunz CMC, Caldini EG, Irigoyen MC. Nicotinamide attenuates streptozotocin-induced diabetes complications and increases survival rate in rats: role of autonomic nervous system. BMC Endocr Disord. 2021; 21:133.

40- Tang WH, Cheng WT, Kravtsov GM, Tong XY, Hou XY, Chung SK, Chung SS. Cardiac contractile dysfunction during acute hyperglycemia due to impairment of SERCA by polyol pathway-mediated oxidative stress. Am J Physiol Cell Physiol. 2010; 299:C643-53.

41- Horáková L, Strosova MK, Spickett CM, Blaskovic D. Impairment of calcium ATPases by high glucose and potential

pharmacological protection. Free Radic Res. 2013; 47:81-92.

42- Abdelazeim SA, Shehata NI, Aly HF, Shams SGE. Amelioration of oxidative stress-mediated apoptosis in copper oxide nanoparticles-induced liver injury in rats by potent antioxidants. Sci Rep. 2020; 10:10812.

43- Laorodphun P, Cherngwelling R, Panya A, Arjinajarn P. Curcumin protects rats against gentamicin-induced nephrotoxicity by amelioration of oxidative stress, endoplasmic reticulum stress and apoptosis. Pharm Biol. 2022; 60:491-500.